PHYSICAL REVIEW B VOLUME 58, NUMBER 20 15 NOVEMBER 1998-II

Metal-insulator transition due to charge ordering in $R_{1/2}Ba_{1/2}CoO_3$

Y. Moritomo
CIRSE and Department of Crystalline Materials Science, Nagoya University, Nagoya 464-8603, Japan and PRESTO, JST, Chiyoda-ku, Tokyo 102, Japan

M. Takeo, X. J. Liu, and T. Akimoto
Department of Crystalline Materials Science, Nagoya University, Nagoya 464-8603, Japan

A. Nakamura
CIRSE and Department of Crystalline Materials Science, Nagoya University, Nagoya 464-8603, Japan

(Received 30 July 1998)

Lattice constants, resistivity, and Raman scattering spectra have been investigated for $R_{1/2}Ba_{1/2}CoO_3$, where R is a trivalent rare-earth ion, with systematically changing the averaged ionic radius r_R of the rare-earth ion. For $R=$Gd, Eu, Sm, prominent metal-insulator (MI) transition is observed at $T_{MI}\sim 360$ K, but the transition is suppressed for $R=$La. The MI transition becomes also blurred for $Gd_{0.48}Ba_{0.52}CoO_3$, suggesting that the transition is due to charge ordering. We have observed enhancement of intensity of Raman scattering from the Co-O stretching mode in the insulating state ($T\leqslant T_{MI}$), and have interpreted it in terms of folding of the oxygen phonon branch due to doubling of the cell size. [S0163-1829(98)51444-0]

A charge-ordering phenomenon, that is, real-space ordering of the doped carriers, is commonly observed in perovskite-type transition-metal oxides when the nominal hole concentration x takes a commensurate value, e.g., $La_{5/3}Sr_{1/3}NiO_4$ ($x=\frac{1}{3}$),[1] $La_{1/2}Sr_{3/2}MnO_4$ ($x=\frac{1}{2}$),[2] and $La_{15/8}Sr_{1/8}CuO_4$ ($x=\frac{1}{8}$).[3] In doped manganites, the charge-ordering transition frequently accompanies significant lattice distortion as well as orderings of spin and orbital (or Jahn-Teller distortion).[2,4–7] For example, $Nd_{1/2}Sr_{1/2}MnO_3$ (Ref. 4) is a conducting ferromagnet ($158\ \text{K}\leqslant T\leqslant 250\ \text{K}$), but is transferred into an antiferromagnetic charge-ordered insulator below ~ 158 K. The transition accompanies significant change of lattice parameters; lattice constant c is reduced by more than 1%, while a and b elongate in the charge-ordered states. The variation of lattice parameters suggests that the charge-ordering transition is coupled with Jahn-Teller instability inherent to the Mn^{3+} ions, or equivalently with the orbital degrees of freedom. Recently, Murakami *et al.*[8] directly observed the charge and orbital ordering for $La_{1/2}Sr_{3/2}MnO_4$ single crystal by means of synchrotron x-ray experiments, which will lead us to *orbital physics*.

In this Communication, we propose another candidate of the charge-ordering material, perovskite-type cobalt oxides $R_{1/2}Ba_{1/2}CoO_3$, where R^{+3} is trivalent rare-earth ions. In the $GdFeO_3$-type distorted perovskite system, reduction of the averaged ionic radius r_A of the perovskite-A site decreases the transfer integral t between the transition-metal sites via variation of the M-O-M bond angle (*chemical pressure* effect[9]). The compounds with smaller rare-earth ions, i.e., $R=$Gd, Eu, and Sm, show a prominent phase transition from metal to insulator at $T_{MI}\sim 360$ K. We have observed enhancement of intensity of Raman scattering from the Co-O stretching vibration, and interpreted it in terms of folding of the phonon branch due to doubling of the cell size in the charge-ordered state. We have investigated effects of chemical substitution of R^{3+} ions on the charge-ordering transition, and have derived an electronic phase diagram.

Melt-grown crystals of $R_{1/2}Ba_{1/2}CoO_3$ ($R=$Gd, Eu, Sm, $Sm_{0.5}Nd_{0.5}$, Nd, $Nd_{0.5}La_{0.5}$ and La) were obtained by the floating-zone method at a feeding speed of 50–60 mm/h. Stoichiometric mixture of commercial Gd_2O_3, Eu_2O_3, Sm_2O_3, Nd_2O_3, La_2O_3, $BaCO_3$, and CoO powder was ground and calcined twice at 1000–1100 °C for 8 h. The resulting powder was pressed into a rod with a size of 5 mm$\phi\times$60 mm and sintered at 1100–1150 °C for 24 h. The ingredient could be melted congruently in a flow of oxygen. Powder x-ray diffraction measurements at room temperature and Rietveld analysis[10] indicate that the crystals were nearly single phase except for $R=$La. The crystal symmetry is found to be orthorhombic ($Pbnm$; $Z=4$) for all the samples investigated.

We show in Fig. 1 a prototypical example of the x-ray powder pattern together with the best-fitted results ($R_{wp}=19.44$; open triangles indicate impurity peaks.). Lattice constants are determined to be $a=5.5284(4)$ Å, $b=5.5336(6)$ Å, and $c=7.5147(3)$ Å. Thus obtained lattice parameters are plotted in Fig. 2 against r_R. The lattice structure for $Gd_{1/2}Ba_{1/2}CoO_3$ is pseudotetragonal with shortened lattice constant c, i.e., $a\approx b\gg c/\sqrt{2}$. With increasing r_R, the c value gradually increases from 7.515 Å for $R=$Gd to 7.631 Å for $R=Nd_{0.5}La_{0.5}$, while a and b remain nearly constant. Such a systematic change of the lattice parameters should affect transport properties of $R_{1/2}Ba_{1/2}CoO_3$. We further measured powder pattern of ceramics sample of $Gd_{1/2}Ba_{1/2}CoO_3$, and found that the lattice symmetry is different from the melt-grown sample; the (1,0,1) and (2,0,2) reflection which locate at $\sim 23°$ and $\sim 47°$, respectively,

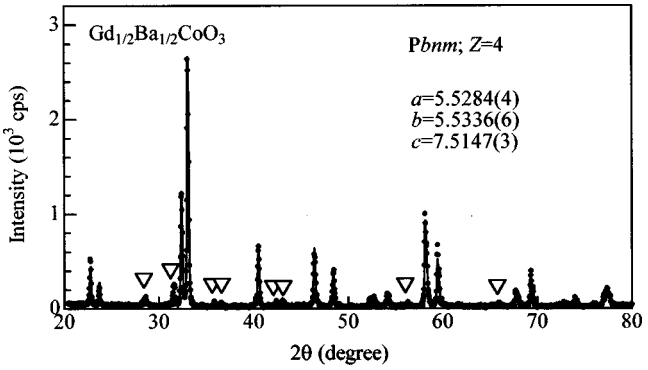

FIG. 1. Powder x-ray pattern (filled circles) for melt-grown $Gd_{1/2}Ba_{1/2}CoO_3$. Solid curve is the result of the Rietveld analysis ($R_{wp}=19.44$). Open triangles indicate impurity peaks.

were split into two reflections, indicating that the symmetry is lower in the ceramics sample.

We show in Fig. 3(a) temperature dependence of resistivity ρ up to ~ 400 K for $R_{1/2}Ba_{1/2}CoO_3$. For four-probe resistivity measurements, the crystal was cut into a rectangular shape, typically of $3\times2\times1\ mm^3$, and electrical contacts were made with a heat-treatment-type silver paint. In the case of $Gd_{1/2}Ba_{1/2}CoO_3$, the $\rho-T$ curve is metallic above $T_{MI}=363$ K, but suddenly jumps and becomes insulating below T_{MI}. Such a resistivity behavior is reminiscent of the charge-ordering transition of $Nd_{1/2}Sr_{1/2}MnO_3$,[4] which shows a charge-ordering transition at $T_{CO}=158$ K. The overall feature of resistivity agrees with the work by Troyanchuk *et al.*,[11] although the resistivity jump at ~ 240 K cannot be reproduced. We further measured resistivity of the ceramics sample (not shown), but could not find the resistivity jump at ~ 240 K. Therefore, we suspect that the resistivity anomaly is not intrinsic but possibly due to some impurities. Hereafter, we will concentrate our attention on the phase transition at T_{MI} ($=363$ K).

The insulating state below T_{MI} is considered to be a charge-ordered state,[12] because the MI transition is fairly suppressed when the nominal hole concentration deviates from the commensurate value ($x=\frac{1}{2}$). The inset of Fig. 3(b) indicates filling dependence of the $\rho-T$ curves for $Gd_{1-x}Ba_xCoO_3$. At $x=0.50$, a definite phase transition is observed at $T_{MI}=363$ K. The phase transition is, however, fairly dimmed at $x=0.52$; a trace of the phase transition is seen at ~ 230 K. Such a behavior is characteristic of charge-ordering transition.[13]

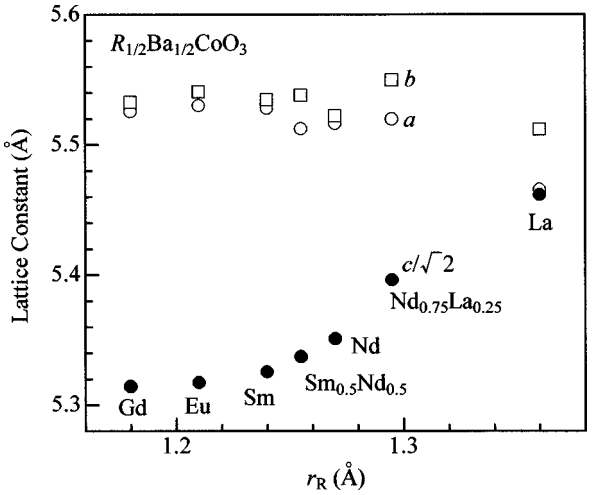

FIG. 2. Lattice constants for $R_{1/2}Ba_{1/2}CoO_3$, where R^{3+} is trivalent rare-earth ions, at 300 K against averaged ionic radius r_R of the rare-earth ion.

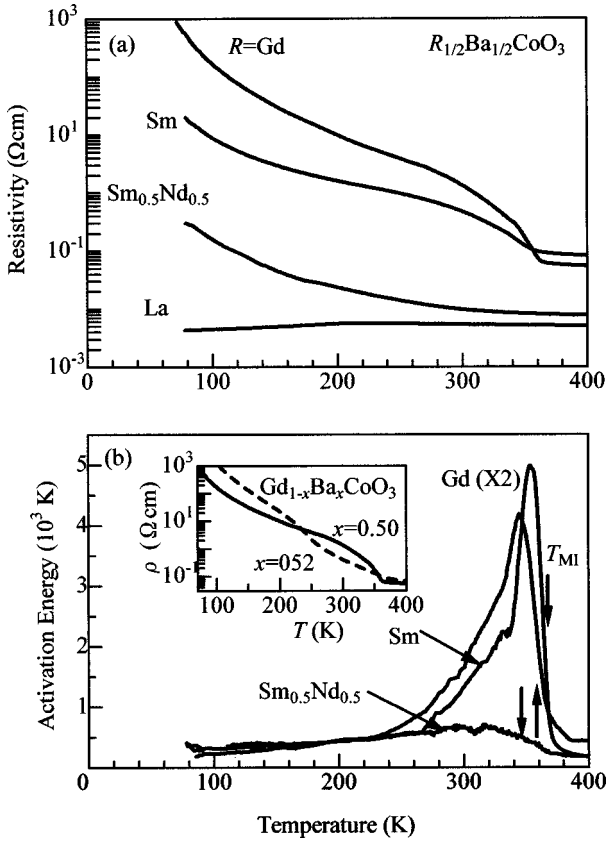

FIG. 3. Temperature dependence of (a) resistivity and (b) activation energy for $R_{1/2}Ba_{1/2}CoO_3$. Arrows in the lower panel indicate the critical temperature T_{MI} for the metal-insulator transition. Inset shows the filling dependence of resistivity for $Gd_{1-x}Ba_xCoO_3$.

The effect of the charge ordering also appears in Raman scattering spectra, which are the most sensitive probes for local symmetry.[14] We show in the inset of Fig. 4 temperature dependence of Raman scattering spectra for $Gd_{1/2}Ba_{1/2}CoO_3$ in the Co-O stretching mode region; solid and broken curves are for the low-temperature ($\leqslant T_{MI}$) and the high-temperature ($\geqslant T_{MI}$) phase, respectively. The melt-grown sample was excited at 514.5 nm with an argon ion laser in a backward configuration. In the high-temperature phase (broken curve), the scattering intensity due to the Co-O stretching vibration is fairly weak, reflecting Raman inactivity of the mode.[15] By contrast, enhancement of the intensity is observed in the insulating state (solid curve). Intensity of the mode was estimated and plotted in Fig. 4. As temperature decreases, the intensity steeply rises around T_{MI} (indicated by an arrow), and continually increases below T_{MI}. The enhancement can be ascribed to the folding of the oxygen phonon branch due to doubling the cell volume in the charge-ordered state.

Now, let us see the lattice effect on the charge-ordering transition. In Fig. 3(a) are shown effects of rare-earth size on

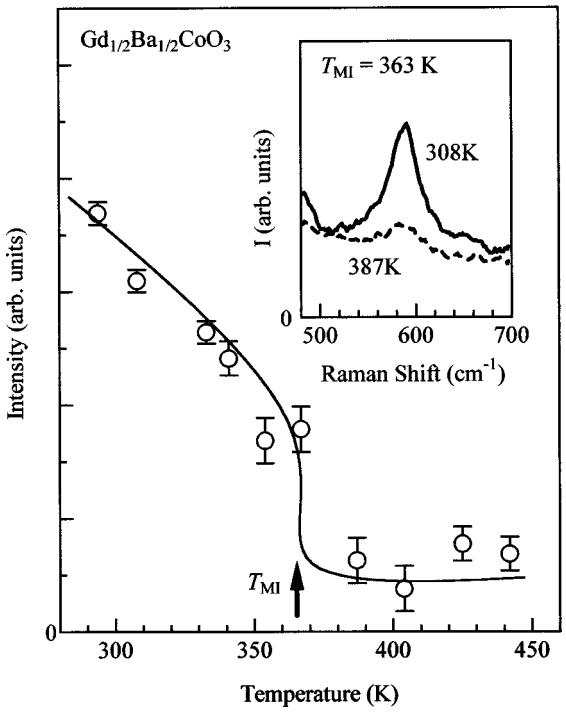

FIG. 4. Temperature dependence of Raman scattering intensity due to the Co-O stretching vibration. Curve is merely a guide to the eyes. T_{MI} is the critical temperature for the metal-insulator transition. Inset shows Raman scattering spectra at 308 K ($\leqslant T_{MI}$) and at 387 K ($\geqslant T_{MI}$).

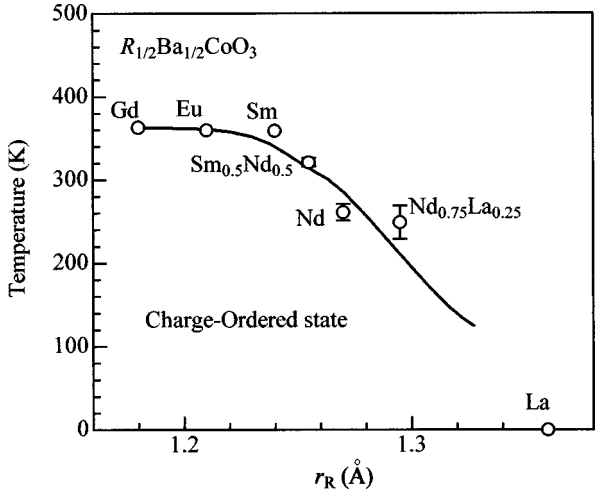

FIG. 5. Electronic phase diagram for $R_{1/2}Ba_{1/2}CoO_3$ against averaged ionic radius r_R of the rare-earth ion. The critical temperatures are determined from the temperature dependence of activation energy E_{ac} (see text).

temperature variation of resistivity. The absolute value of resistivity decreases as r_R increases from $R=$Gd to La, reflecting release of the $GdFeO_3$-type distortion (*chemical pressure* effect; see also Fig. 2). Accordingly, the charge-ordering transition becomes blurred; the transition is barely discernible for $R=$Sm in the $\rho-T$ curve. In the case of $R=$La, the charge-ordering transition disappears and a metallic resistivity is observed down to $\sim$80 K. In order to precisely determine the charge-ordering temperature T_{MI}, we plotted in Fig. 3(b) temperature variation of activation energy E_{ac}, which is defined by

$$E_{ac}=dln(\rho)/d(1/T). \quad (1)$$

Steep rise of E_{ac} is observed at $T_{MI}=363$ K for $R=$Gd and $T_{MI}=361$ K for $R=$Sm. The rise, however, becomes burred in $R=Sm_{0.5}Nd_{0.5}$, reflecting gradual change of the electronic and lattice structure. So, we tentatively defined T_{MI} as the temperature where the E_{ac} value becomes half of the maximum value. Thus obtained critical temperatures for the charge-ordering transition are plotted in Fig. 5 against r_R. With increasing r_R value, T_{MI} gradually decreases, and eventually the transition vanishes at $r_R=1.36$ Å ($R=$La). In addition, character of the transition changes with r_R as well. Steep rises of ρ and E_{ac} are observed in the small-r_R region, reflecting first-order nature of the transition. In fact, we observed thermal hysteresis of $\sim$4 K for $Gd_{1/2}Ba_{1/2}CoO_3$ around $T_{MI}=363$ K. The transition, however, becomes dimmed as r_R increases, suggesting that the transition is of second-order or of crossover-type.

Finally, let us comment on the interrelation between the charge-ordering transition and lattice structure. Troyanchuk *et al.*[16] have observed a significant reduction of the crystallographic c axis of more than 2% at the metal-insulator transition. Such a reduction of c is advantageous to the charge-ordered insulating state because the resultant lattice distortion reduces the transfer integral t between the Co sites. This also explains why the charge-ordered state is stable in the small-c compound, e.g., $R=$Gd, Eu, and Sm (see Fig. 2 and Fig. 5) However, we should recall that the Co^{3+} (d^6) ion can take the intermediate spin (IS; $S=1$) state in oxide system.[17] Then, it is probable that the charge-ordered state is stabilized by a cooperative Jahn-Teller distortion of $Co^{3+}O_6$ octahedra within the ab plane. In this sense, the present cobalt oxide system is analogous to the prototypical charge-ordering material $Nd_{1/2}Sr_{1/2}MnO_3$, in which cooperative Jahn-Teller distortion of $Mn^{3+}O_6$ octahedra (or the orbital ordering) results in shrinkage of c more than 1%.

In summary, we have systematically investigated the lattice constant and resistivity for $R_{1/2}Ba_{1/2}CoO_3$, where R^{3+} is a trivalent rare-earth ion. In smaller R^{3+} region, the compounds show prominent metal-insulator (MI) transition at $T_{MI}\sim 360$ K. The MI transition becomes blurred when the nominal hole concentration deviates from a commensurate value. We further found significant enhancement of the Raman scattering intensity due to the Co-O stretching vibration in the insulating state ($\leqslant T_{MI}$), and interpreted it in terms of folding of the oxygen phonon branch. These results suggest that the low-temperature insulating state is a charge-ordered state. Detailed x-ray diffraction measurements as well as electron diffraction measurements are now in progress to determine the pattern of the charge ordering.

The authors are grateful to S. Mori and C.-H. Chen for fruitful discussions. This work was supported by a Grant-in-Aid for Scientific Research from the Ministry of Education, Science and Culture, Japan, and also from Precursory Research for Embryonic Science and Technology (PRESTO), Japan Science and Technology Cooperation (JST), Japan.

[1] S.-W. Cheong, H.-Y. Hwang, C.-H. Chen, B. Batlogg, L. W. Ruppa, Jr., and S. A. Carter, Phys. Rev. B **49**, 7088 (1994).

[2] Y. Moritomo, Y. Tomioka, A. Asamitsu, and Y. Tokura, Phys. Rev. B **51**, 3297 (1995); Y. Moritomo, A. Nakamura, S. Mori, Y. Yamamoto, K. Ohoyama, and M. Ohashi, *ibid.* **56**, 14 879 (1997).

[3] J. M. Tranquada, B. J. Sternlieb, J. D. Axe, Y. Nakamura, and S. Uchida, Nature (London) **337**, 561 (1995).

[4] H. Kuwahara, Y. Tomioka, A. Asamitsu, Y. Moritomo, and Y. Tokura, Science **270**, 961 (1995).

[5] Y. Moritomo, H. Kuwahara, Y. Tomioka, and Y. Tokura, Phys. Rev. B **55**, 7549 (1997).

[6] H. Kuwahara, Y. Moritomo, Y. Tomioka, A. Asamitsu, M. Kasai, R. Kumai, and Y. Tokura, Phys. Rev. B **56**, 9386 (1997).

[7] J. Q. Li, Y. Matsui, T. Kimura, and Y. Tokura, Phys. Rev. B **57**, R3205 (1998).

[8] Y. Murakami, H. Kawada, H. Kawata, T. Tanaka, T. Arima, Y. Moritomo, and Y. Tokura, Phys. Rev. Lett. **80**, 1932 (1998).

[9] For example, see P. G. Radaelli, G. Iannone, M. Marezio, H. Y. Hwang, S.-W. Cheong, J. D. Jorgensen, and D. N. Argyriou, Phys. Rev. B **56**, 8265 (1997).

[10] F. Izumi, in *The Rietveld Method*, edited by R. A. Young (Oxford University Press, Oxford, England, 1993), Chap. 13; Y.-I. Kim and F. Izumi, J. Ceram. Soc. Jpn. **102**, 401 (1994).

[11] I. O. Troyanchuk, N. V. Kasper, D. D. Khalyavin, H. Szymczak, R. Szymczak, and M. Baran, Phys. Rev. Lett. **80**, 3380 (1998).

[12] (1/2,0,0) superlattice reflection has been observed in the electron diffraction pattern for $Gd_{1/2}Ba_{1/2}CoO_3$ at 300 K ($\leqslant T_{MI}$). This suggests charge-ordering, i.e., alternating of the Co^{3+} and Co^{4+} species within the ab plane, in the low-temperature phase [S. Mori *et al.*, (unpublished)].

[13] Y. Moritomo, T. Akimoto, A. Nakamura, K. Ohoyama, and M. Ohashi, Phys. Rev. B **58**, 5544 (1998).

[14] For example, see Y. Moritomo, Y. Tokura, N. Nagaosa, T. Susuki, and K. Kumagai, Phys. Rev. Lett. **71**, 2833 (1993).

[15] The enumeration of the oxygen vibration is $\Gamma = 2T_{1u} + T_{2u}$ in the simple cubic perovskite (space group O_h).

[16] I. O. Troyanchuk, N. V. Kasper, D. D. Khalyavin, H. Szymczak, R. Szymczak, and M. Baran, Phys. Rev. B **58**, 2418 (1998).

[17] Y. Moritomo, K. Higashi, K. Matsuda, and A. Nakamura, Phys. Rev. B **55**, R14 725 (1997), and references cited therein.